

Integration radius as a parameter separating convergent and divergent spherical harmonic series of topography-implied gravity

Blažej Bucha¹ Michael Kuhn²

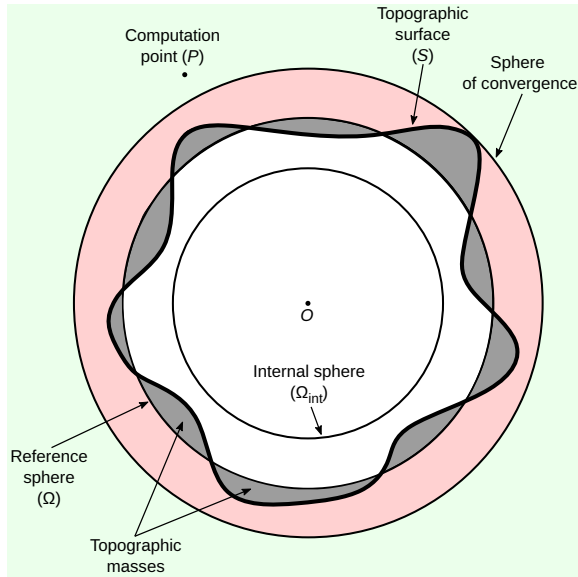
¹Department of Theoretical Geodesy and Geoinformatics
Slovak University of Technology in Bratislava
blazej.bucha@stuba.sk

²Western Australian Geodesy Group, School of Earth and Planetary Sciences, Curtin University, GPO Box U1987, Perth, WA 6845, Australia
m.kuhn@curtin.edu.au

IUGG Berlin 2023

Motivation

Global spectral gravity forward modelling



Global forward modelling:

$$\bar{H}_{nm} \longrightarrow \bar{V}_{nm}$$

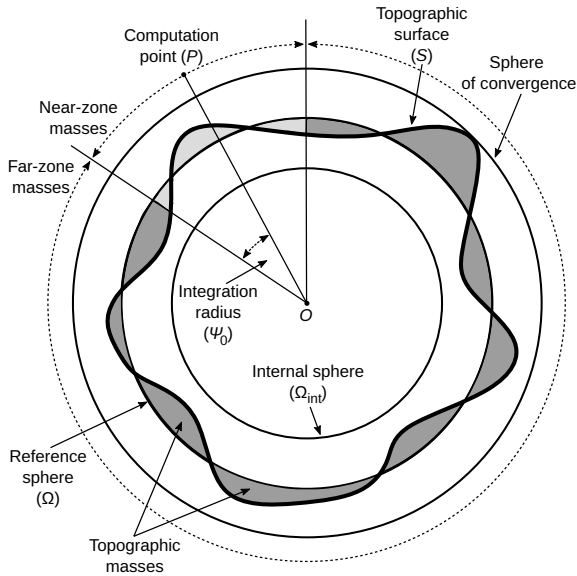
Potential series:

$$V = \frac{GM}{R} \sum_{n=0}^{\infty} \left(\frac{R}{r} \right)^{n+1} \times \sum_{m=-n}^{n} \bar{V}_{nm} \bar{Y}_{nm}(\varphi, \lambda)$$

Series behaviour:

- Convergence guaranteed
- Convergence not guaranteed

Cap-modified spectral gravity forward modelling



Cap-modified forward modelling:

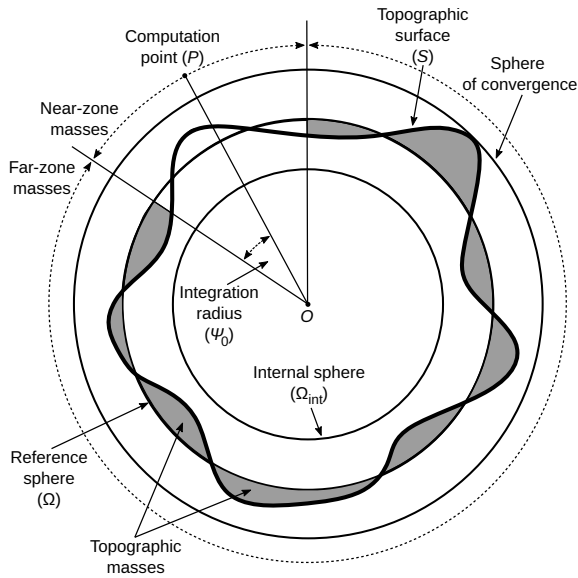
$$\bar{H}_{nm} \longrightarrow \bar{V}_{nm}^j(r, \psi_0)$$

with $j = \text{'N'}$ (near-zone) or
‘F’ (far-zone).

Potential series:

$$V^j = \frac{GM}{R} \sum_{n=0}^{\infty} \sum_{m=-n}^n \bar{V}_{nm}^j(r, \psi_0) \times \bar{Y}_{nm}(\varphi, \lambda)$$

Far-zone effects



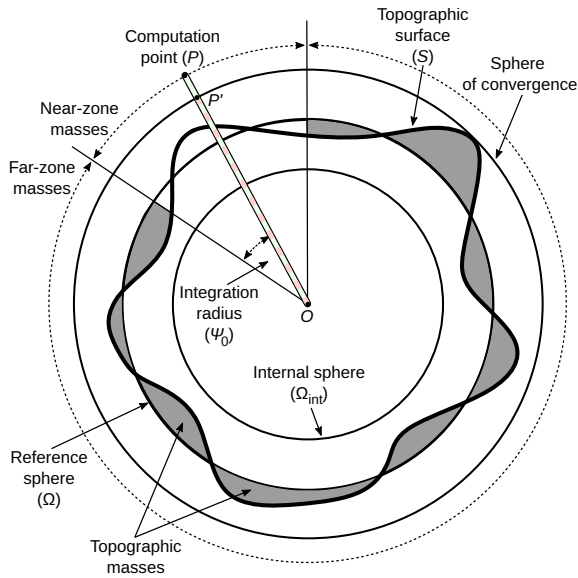
Cap-modified forward modelling:

$$\bar{H}_{nm} \longrightarrow \bar{V}_{nm}^F(r, \psi_0)$$

Potential series:

$$V^F = \frac{GM}{R} \sum_{n=0}^{\infty} \sum_{m=-n}^n \bar{V}_{nm}^F(r, \psi_0) \times \bar{Y}_{nm}(\varphi, \lambda)$$

Far-zone effects



Cap-modified forward modelling:

$$\bar{H}_{nm} \longrightarrow \bar{V}_{nm}^F(r, \psi_0)$$

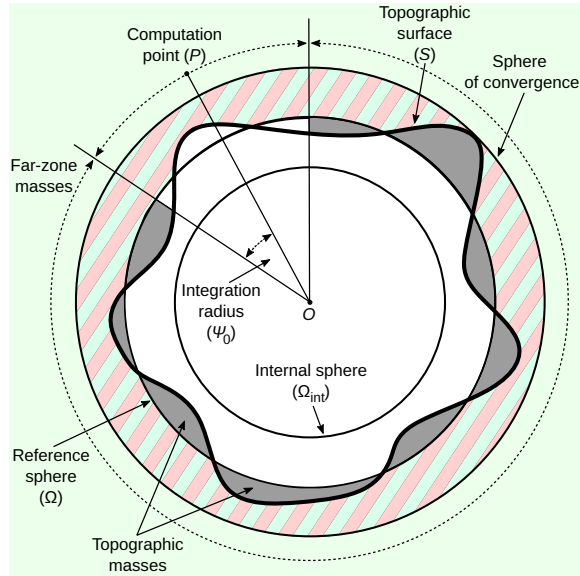
Potential series:

$$V^F = \frac{GM}{R} \sum_{n=0}^{\infty} \sum_{m=-n}^n \bar{V}_{nm}^F(r, \psi_0) \times \bar{Y}_{nm}(\varphi, \lambda)$$

Convergence on $\overline{PP'}$.

But what about $\overline{P'O}$?

Far-zone effects



What is the convergence region for far-zone effects?

Theory

Formulation of the problem

- For a constant mass density and $r_S > R_{\text{int}}$, Newton's integral reads:

$$V^F(r, \varphi, \lambda) = G \rho \int_{\psi=\psi_0}^{\pi} \int_{\alpha=0}^{2\pi} \int_{r'=R_{\text{int}}}^{r_S} \frac{(r')^2}{\ell(r, \psi, r')} dr' d\alpha \sin \psi d\psi. \quad (1)$$

Formulation of the problem

- For a constant mass density and $r_S > R_{\text{int}}$, Newton's integral reads:

$$V^F(r, \varphi, \lambda) = G \rho \int_{\psi=\psi_0}^{\pi} \int_{\alpha=0}^{2\pi} \int_{r'=R_{\text{int}}}^{r_S} \frac{(r')^2}{\ell(r, \psi, r')} dr' d\alpha \sin \psi d\psi. \quad (1)$$

- Taylor expansion of Newton's kernel [Martinec(1998)]:

$$\frac{(r')^2}{\ell(r, \psi, r')} = R_{\text{int}}^2 \sum_{i=0}^{\infty} \frac{1}{i!} M_i(r, \psi, R_{\text{int}}) \left(\frac{r' - R_{\text{int}}}{R_{\text{int}}} \right)^i. \quad (2)$$

Formulation of the problem

- For a constant mass density and $r_S > R_{\text{int}}$, Newton's integral reads:

$$V^F(r, \varphi, \lambda) = G \rho \int_{\psi=\psi_0}^{\pi} \int_{\alpha=0}^{2\pi} \int_{r'=R_{\text{int}}}^{r_S} \frac{(r')^2}{\ell(r, \psi, r')} dr' d\alpha \sin \psi d\psi. \quad (1)$$

- Taylor expansion of Newton's kernel [Martinec(1998)]:

$$\frac{(r')^2}{\ell(r, \psi, r')} = R_{\text{int}}^2 \sum_{i=0}^{\infty} \frac{1}{i!} M_i(r, \psi, R_{\text{int}}) \left(\frac{r' - R_{\text{int}}}{R_{\text{int}}} \right)^i. \quad (2)$$

- Substituting Eq. (2) into (1), **interchanging the order of the summation and integrations** and after some derivations, we get:

$$V^F(r, \varphi, \lambda) = \frac{GM}{R} \sum_{n=0}^{\infty} \sum_{m=-n}^n \bar{V}_{nm}^F(r, \psi_0) \bar{Y}_{nm}(\varphi, \lambda). \quad (3)$$

Formulation of the problem

- The summation and integrations can be interchanged only if the Taylor series (2) converges uniformly. [Martinec(1998)] has shown that the radius of convergence of (2) for $r = R_{\text{int}}$ is ℓ . This implies

$$\psi_0 > 2 \arcsin \left(\frac{\max(\hat{H}_{\text{int}}(\varphi', \lambda'))}{2 R_{\text{int}}} \right) \approx \frac{\max(\hat{H}_{\text{int}}(\varphi', \lambda'))}{R_{\text{int}}}. \quad (4)$$

Formulation of the problem

- The summation and integrations can be interchanged only if the Taylor series (2) converges uniformly. [Martinec(1998)] has shown that the radius of convergence of (2) for $r = R_{\text{int}}$ is ℓ . This implies

$$\psi_0 > 2 \arcsin \left(\frac{\max(\hat{H}_{\text{int}}(\varphi', \lambda'))}{2 R_{\text{int}}} \right) \approx \frac{\max(\hat{H}_{\text{int}}(\varphi', \lambda'))}{R_{\text{int}}}. \quad (4)$$

- The radius of convergence for $r > R_{\text{int}}$ is not known.

Formulation of the problem

- The summation and integrations can be interchanged only if the Taylor series (2) converges uniformly. [Martinec(1998)] has shown that the radius of convergence of (2) for $r = R_{\text{int}}$ is ℓ . This implies

$$\psi_0 > 2 \arcsin \left(\frac{\max(\hat{H}_{\text{int}}(\varphi', \lambda'))}{2 R_{\text{int}}} \right) \approx \frac{\max(\hat{H}_{\text{int}}(\varphi', \lambda'))}{R_{\text{int}}}. \quad (4)$$

- The radius of convergence for $r > R_{\text{int}}$ is not known.
- Hypothesis:** The radius of convergence of the Taylor series (2) for $r \geq R_{\text{int}}$ is ℓ .
This implies

$$\psi_0 > \arccos \left(\frac{r^2 + R_{\text{int}}^2 - (\max(\hat{H}_{\text{int}}))^2}{2 r R_{\text{int}}} \right). \quad (5)$$

- If (5) is satisfied and if the hypothesis is true, then we have a proof that external spherical harmonic expansions of far-zone gravitational effects converge *even on the topography and below it down to the R_{int} -sphere.*

- If (5) is satisfied and if the hypothesis is true, then we have a proof that external spherical harmonic expansions of far-zone gravitational effects converge *even on the topography and below it down to the R_{int} -sphere.*
- The hypothesis has not yet been proven. The main obstacle is the form of the kernels M_i ,

$$\begin{aligned}
 M_i(r, \psi, R_{\text{int}}) = & \frac{1}{\ell} \sum_{s=1}^{i-1} \frac{i! (i-2)!}{(i-s-1)! (s-1)!} \left(\frac{r}{\ell}\right)^{i+1-s} \\
 & \times \sum_{t=0}^{i+1-s} (-1)^{\frac{1}{2}(3i+1-s+t)} \frac{(i+2-s-t)!! (i-s+t)!!}{(i+2-s-t)! t!} \\
 & \times \left(\frac{z}{\ell}\right)^t.
 \end{aligned} \tag{6}$$

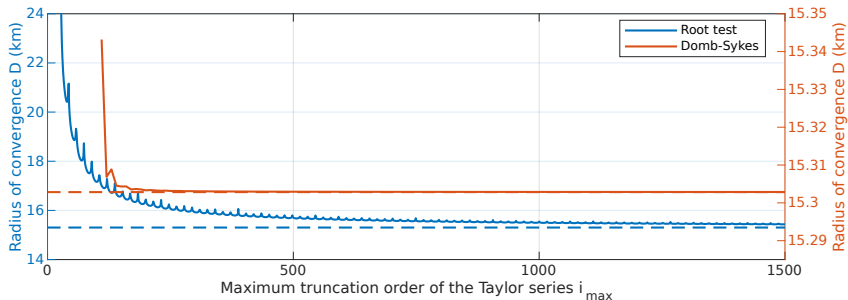
Numerical experiments

Radius of convergence of the TS: Numerical approach

Using the root test $C = \limsup_{i \rightarrow \infty} \sqrt[i]{|c_i|}$, the radius of convergence is $D = \frac{1}{C}$.

Radius of convergence of the TS: Numerical approach

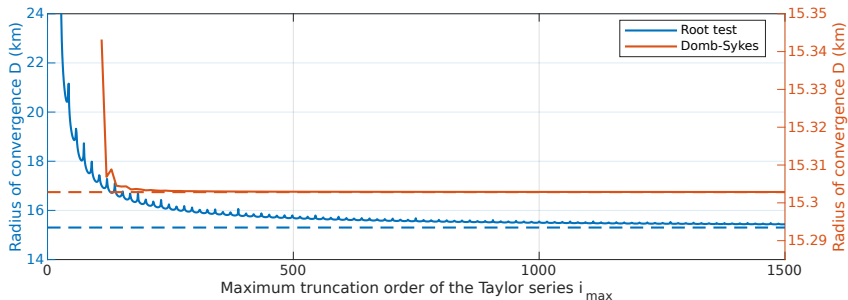
Using the root test $C = \limsup_{i \rightarrow \infty} \sqrt[i]{|c_i|}$, the radius of convergence is $D = \frac{1}{C}$.



Radius of convergence of the Taylor series (2) for $r = R_{\text{int}} + 15,000$ m, $\psi_0 = 0.1^\circ$ and $R_{\text{int}} = 1,728,200$ m. Both methods have their own vertical axis, given that the Domb–Sykes method converges significantly faster. For each axis, shown is also the (same) prediction of the radius of convergence ℓ (dashed lines).

Radius of convergence of the TS: Numerical approach

Using the root test $C = \limsup_{i \rightarrow \infty} \sqrt[i]{|c_i|}$, the radius of convergence is $D = \frac{1}{C}$.

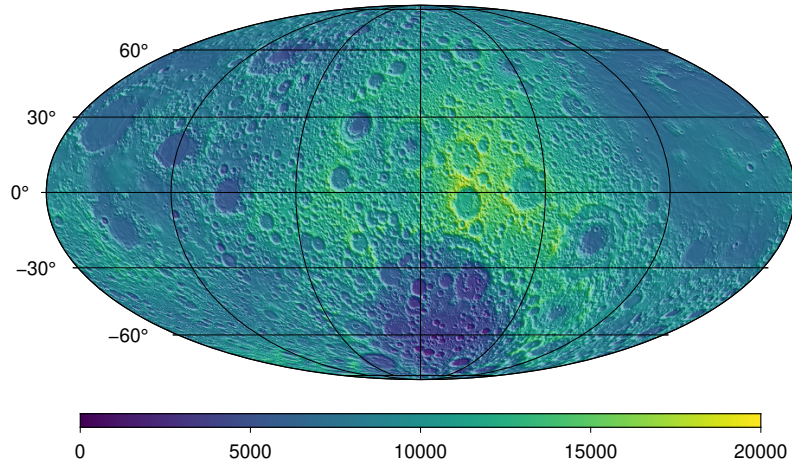


Radius of convergence of the Taylor series (2) for $r = R_{\text{int}} + 15,000$ m, $\psi_0 = 0.1^\circ$ and $R_{\text{int}} = 1,728,200$ m. Both methods have their own vertical axis, given that the Domb–Sykes method converges significantly faster. For each axis, shown is also the (same) prediction of the radius of convergence ℓ (dashed lines).

The numerical experiments do not invalidate the hypothesis.
This is far from a formal proof, though.

Design of the experiment

Gravitating body: Moon's topographic masses up to degree 2160.

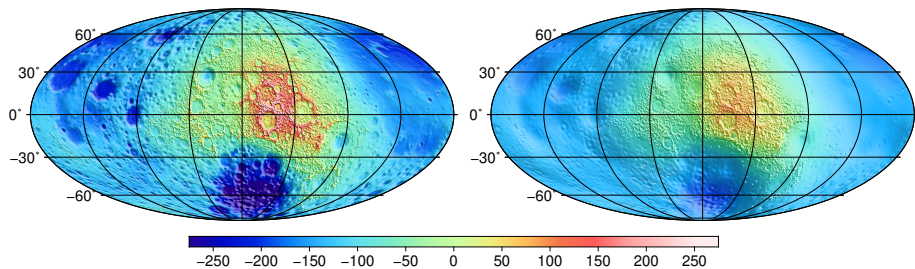


Moon's topographic heights (m) referenced to the sphere of radius $R_{\text{int}} = 1,728,200$ m.

Design of the experiment

Reference gravity disturbances: Spatial-domain forward modelling for several ψ_0 , the threshold being $\approx 0.663^\circ$ (≈ 20.114 km).

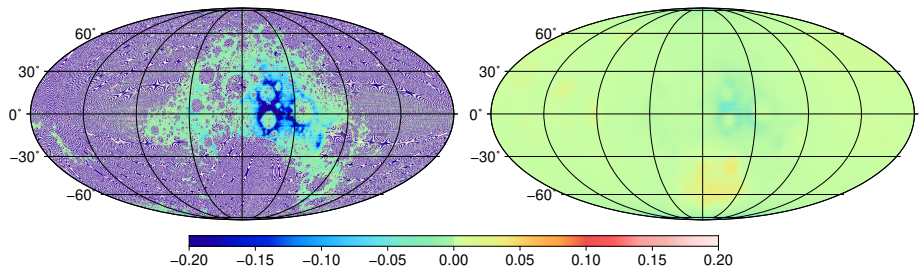
| ℓ_0 (km) | 2.5 | 5.0 | 7.5 | 10.0 | 12.5 | 15.0 | 20.0 | 30.0 | 50.0 | 100.0 |
|---------------------------|------|------|------|------|------|------|-------|------|------|-------|
| $\psi_0 = \ell_0/R$ (deg) | 0.08 | 0.16 | 0.25 | 0.33 | 0.41 | 0.49 | 0.659 | 0.82 | 1.65 | 3.30 |
| Series behaviour | D | D | D | D | D | D | D | C | C | C |



*Reference far-zone gravity disturbances (mGal) from a divergence-free spatial-domain Newtonian integration residing on the surface of the field-generating masses.
Left: $\ell_0 = 10$ km, right $\ell_0 = 50$ km.*

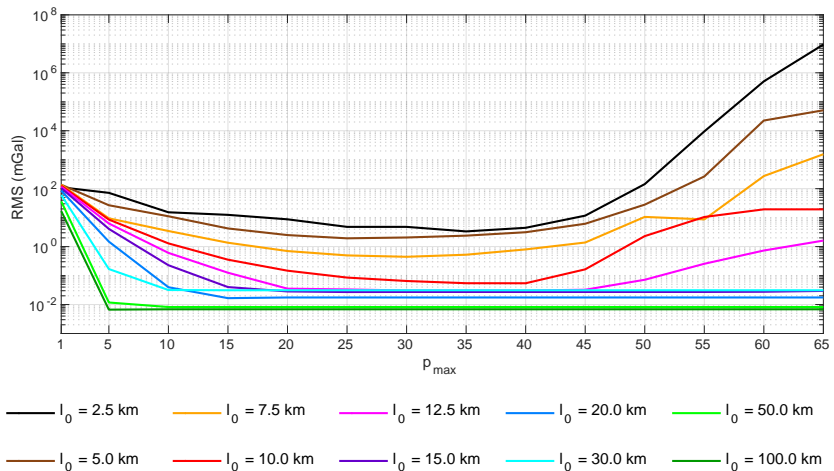
Results

- Maximum harmonic degree of the potential series: 10,800
- Number of topography powers: 65



Differences between spectral- and spatial-domain far-zone gravity disturbances (mGal) on the surface of the field-generating masses. Left: $\ell_0 = 10$ km, right $\ell_0 = 50$ km. The discrepancies on the left reach thousands of mGal.

Results



Differences between spectral- and spatial-domain far-zone gravity disturbances on the surface of the field-generating masses for various integration radii ℓ_0 as a function of the maximum topography power p_{\max} . For $p_{\max} = 1$, the maximum harmonic degree is 2160 and 10,800 otherwise.

Conclusions

Conclusions

- Insights into convergence/divergence of spherical harmonics
- We formulated a hypothesis that separates between convergent and divergent far-zone spherical harmonic series
- Numerical experiments do not invalidate the hypothesis
- Rigorous proof still missing
- Applications in full-scale high-resolution gravity forward modelling:
 - Near-zone effects with spatial methods
 - Far-zone effects with spectral methods

References

-  Z. Martinec.
Boundary-Value Problems for Gravimetric Determination of a Precise Geoid.
Springer-Verlag, Berlin, Heidelberg, 1998.

Thank you
for your attention!

Published in: Bucha, B., Kuhn, M., 2020. *A numerical study on the integration radius separating convergent and divergent spherical harmonic series of topography-implied gravity*. Journal of Geodesy 94, 112, <https://link.springer.com/article/10.1007/s00190-020-01442-z>

Fast high-degree SHA/SHS library in C/Python: www.charmlib.org